Surface Science 278 (1992) 51–61
North-Holland

surface science

Surface chemistry of hydrazine on Pt(111)

Diann J. Alberas, J. Kiss [1], Z.-M. Liu and J.M. White
Department of Chemistry and Biochemistry, University of Texas at Austin, Austin, TX 78712, USA

Received 27 January 1992; accepted for publication 4 July 1992

The thermal decomposition of hydrazine, N_2H_4, adsorbed on a Pt(111) surface at 60 K has been investigated by temperature programmed desorption (TPD), high resolution electron energy loss spectroscopy (HREELS), X-ray photoelectron spectroscopy (XPS), ultraviolet photoelectron spectroscopy (UPS), and temperature programmed secondary ion mass spectroscopy (TPSIMS). Condensed multilayer and chemisorbed states of hydrazine can be distinguished. Submonolayer hydrazine coverages start to decompose between 150 and 200 K by dissociation of N–H, not N–N, bonds. In TPD, H_2, NH_3, and N_2 all peak near 310 K. N_2 and NH_3 desorb in processes limited by the rates of the reactions forming them. N_2 is formed by an *intramolecular* process. No nitrogen containing species are detected above 400 K in HREELS or XPS. Depending on the surface coverage and temperature, dihydrogen desorption is probably limited by both the recombination rate and the rate of N–H cleavage. We propose that: (1) the low temperature N–H bond cleavage and the retention of N–N bonds are facilitated by the chemisorption of N_2H_4 through both nitrogen atoms, and (2) relative to the N–metal bond, the H–metal bond is stronger on Pt(111). As a result, the barrier to N–H cleavage is lowered much more than the barrier to N–N cleavage, and the former is preferred.

1. Introduction

The adsorption and decomposition of hydrazine has been studied on several metal surfaces [1–14]. According to these reports, decomposition can occur by a number of different paths, depending on the metal. In one path, the N–N bond breaks first, leaving NH_2 species on the surface. These typically decompose to N and H, which, upon thermal activation, recombine to desorb N_2 and H_2. In a second path, the NH_2 species react with H to desorb NH_3. In a third path, the N–H bonds break first, forming species such as N_2H_3, N_2H_2, N_2H, and N_2. In this case, N_2 is formed intramolecularly, not by N atom recombination. In a fourth path, hydrazine is directly hydrogenated in a concerted reaction to form ammonia.

Different combinations of these paths have been invoked on different surfaces. For example, on Fe(111) [4] and Al foil [6], only the first path is reported. On Rh(111) [13], all the paths are reported depending on the concentration (coverage) of surface fragments. For example, on Rh foil [14], at low coverages, the first path is reported, whereas at high coverages, all paths are reported.

In this paper, we report a study of the thermal decomposition of hydrazine on Pt(111) using a variety of characterization tools to confirm the operative reaction pathways. We find that, at all coverages, decomposition occurs by N–H, not N–N, bond breaking. Thus, N_2 forms intramolecularly. Ammonia is formed by hydrogenation of N_2H_x. A model is proposed in which the strength of the N–metal, as compared to the N–N and N–H bonds, plays an important role in determining the decomposition path.

2. Experimental

The experiments were carried out in two ultra-high ($(2–3)\times 10^{-10}$ Torr) vacuum cham-

[1] Permanent address: Reaction Kinetics Research Group of the Hungarian Academy of Sciences, University of Szeged, P.O. Box 105, Szeged, Hungary.

bers. One chamber was equipped with a low temperature sample holder (50 K), photoelectron spectroscopy (XPS, UPS) and temperature programmed desorption (TPD) capabilities [15]. The second chamber houses high resolution electron energy loss spectroscopy (HREELS), temperature programmed secondary ion mass spectroscopy (TPSIMS) and Auger electron spectroscopy (AES) facilities, also described elsewhere [16].

HREELS measurements were carried out with a primary beam energy of 6.1 eV and a resolution of 10–12 mV full width at half maximum (FWHM). In XPS measurements, a Mg Kα source was used and the analyzer was set for 80 eV pass energy and 0.1 eV step size. TPD and TPSIMS were performed with a temperature ramping rate of 6 and 4.5 K/s, respectively. An 800 eV Ar^+ beam, and a beam flux of 5–30 nA/cm^2 was used for SIMS. The temperature was measured with a chromel–alumel thermocouple spotwelded to the back of the sample.

The Pt(111) crystal was cleaned by sputtering with Ar^+ or Ne^+, and by oxidation at 900–1000 K in O_2 ($\sim 5 \times 10^{-8}$ Torr) to remove carbon and annealing to 1200 K for several minutes to remove residual oxygen. The surface cleanliness was checked by AES and XPS.

Hydrazine (Aldrich Chemical Corporation) was dosed from a glass tube via a capillary doser attached to a variable leak valve. Many cycles of freezing and thawing in liquid nitrogen and CO_2/acetone were used to remove impurities. To minimize hydrazine decomposition before adsorption, the dosing system was carefully preconditioned by exposure to N_2H_4. Mass spectral analysis, showing only N_2H_4 fragments, was realized after extensive preconditioning. To maintain this condition, we replaced the hydrazine in the dosing manifold between every experiment.

In the chamber containing the low temperature (50 K) sample holder, the cleanliness of the incoming N_2H_4 can be checked by an alternative route. If hydrazine decomposes in the doser, the Pt(111) crystal will be dosed with a multilayer mixture of molecular H_2, N_2, and NH_3 gases. These can be distinguished on the basis of their N(1s) XPS signals, e.g., N_2 at 402.7 eV [17], and NH_3 at 399.9 eV [18]. For the material, purified and dosed as described above, these species were not detectable.

Relative exposures were reproducibly achieved using the following procedure: with the sample turned away from the doser tube, the leak valve was opened to give a predetermined pressure rise at the system ion gauge. To initiate dosing, the sample was turned quickly to intercept the flux from the doser tube. While absolute fluxes to the sample are not known, relative fluxes are reproducible. As outlined below, monolayer coverage is defined in terms of the dose required to observe the onset of multilayer desorption.

3. Results

3.1. TPD

The TPD products observed after dosing N_2H_4 on clean Pt(111) at 60 K are N_2H_4, N_2, H_2, and NH_3 (figs. 1–4, respectively). For N_2H_4 (monitored at 32 amu), there is no signal at low N_2H_4 exposures (0, 10, 20 s), i.e., all the hydrazine thermally decomposes. A broad desorption starting at 200 and ending at 300 K is observed after a 30 s dose. This peak is saturated at 40 s and a new peak at $T_p = 213$ K appears, which shifts down to 205 K and saturates at a 60 s dose. The 205 K peak is attributed to the desorption of the chemisorbed hydrazine monolayer; its saturation is taken as the definition of one monolayer. The shape of the hydrazine desorption spectra is similar to that of ammonia on Pt(111) [18]. At low coverages of ammonia, there is also a broad desorption peak at 350 K attributed to strong charge transfer interactions between the nitrogen lone pair and the surface [18]. We argue against this for the case of hydrazine because unlike ammonia, hydrazine thermally decomposes. Also, there is no other evidence that there are two types of species on the surface. We speculate that the broad higher temperature desorption is attributable to the recombination of H with N_2H_x to reform hydrazine. A third low temperature desorption peak at 167 K is observed at dose times > 40 s. This peak does not saturate and is attributed to the desorption of multilayer N_2H_4.

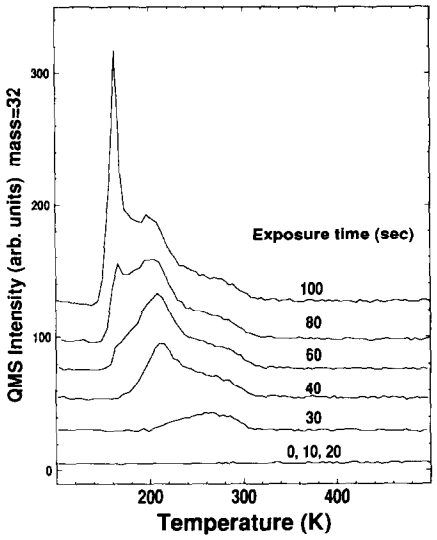

Fig. 1. TPD spectra for various hydrazine exposures on clean Pt(111). To prepare the system, clean Pt(111) was exposed to an unknown, but reproducible, flux of N_2H_4 from a preconditioned pinhole doser. The flux was chosen to give monolayer coverage in about 60 s (see curves). The adsorption temperature was 60 K and the temperature ramp was 6 K/s. (Same in other TPD figures.)

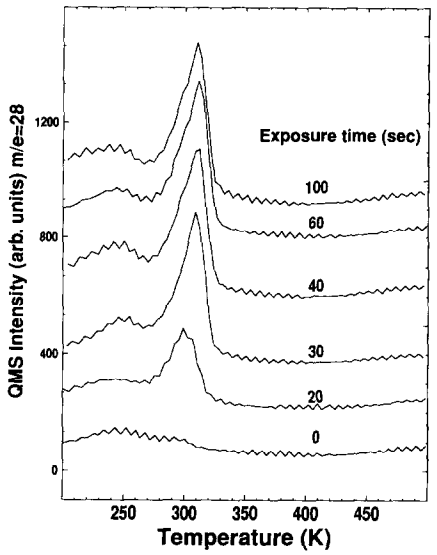

Fig. 2. TPD spectra for N_2 from various hydrazine exposures on clean Pt(111). Conditions were identical to those of fig. 1.

Comparing the above results to those on other metals, we note the following. On Rh(100) [9], the chemisorbed state peaks at 220 and the multilayer at 190 K. On Rh foil at high coverages, there is a peak at 220 K [14], and on Ni(111), multilayer and chemisorbed hydrazine desorption occurs between 150 and 250 K [8]. Our results for Pt(111) fit nicely into this pattern.

Desorption of N_2 (fig. 2) is observed for all doses. It begins at 275 K, ends at 325 K, and reaches a maximum at 310 K. A comparison of 28 and 14 amu (not shown) confirms that the peaks are from N_2, not CO. Interestingly, no high temperature desorption of N_2, typical of N atom recombination, is detected. When N_2 is dosed at 50 K, previous results show that it desorbs at 60 K without dissociation [17,19]. On the other hand, when atomic nitrogen is dosed at low temperatures (< 200 K), it recombines and desorbs as N_2 between 450 and 650 K [20–22]. We conclude that the N_2 observed here is limited by neither desorption of N_2 nor by N atom recombination, i.e., some other reaction limited process controls the rate. This behavior differs from that on Ir(111) [5], Rh(111) [13], Rh(100) [9], Ir foil [2], and Rh foil [14] where there is some high temperature recombination of atomic nitrogen.

Desorption of H_2 (fig. 3) begins at 270 K, goes through a maximum at 310 K, and ends at 360 K,

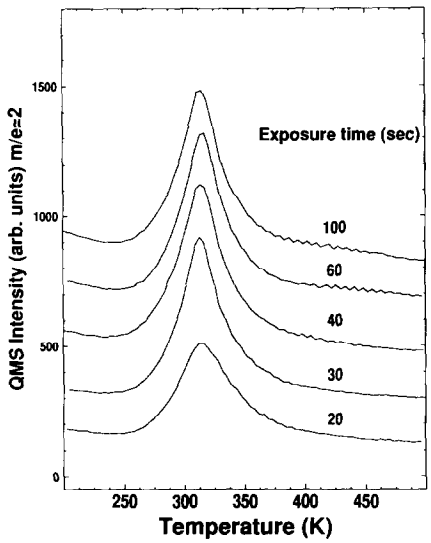

Fig. 3. TPD spectra for H_2 from various hydrazine exposures on clean Pt(111). Conditions were identical to those of fig. 1.

i.e., tracks N_2 desorption reasonably well, but not precisely. In particular, the trailing edge of the H_2 desorption extends to higher temperatures. When H_2 is dosed on Pt(111), H is formed and it recombines and desorbs between 200 and 390 K, depending on the coverage [23]. HREELS and XPS confirm that partial dissociation of parent molecules occurs between 150 and 200 K (see below). Thus, we cannot conclude whether the H_2 peak is controlled by H atom recombination or by N–H dissociation. Likely, each is controlling, but in different coverage-temperature regimes.

There is a sharp NH_3 desorption peak at $T_p = 310$ K (fig. 4), the shape of which differs from TPD of dosed NH_3. Very low coverages of NH_3 adsorbed on clean Pt(111) at 100 K desorb as a very broad peak above 250 K [18]. With increasing NH_3 coverage, the desorption broadens toward lower temperatures, a new feature attributed to monolayer desorption grows in near 160 K and the multilayer desorbs at 110 K. We have reproduced these TPD features in our own work. Thus, the NH_3 arising from N_2H_4 TPD must be the result of a reaction-limited process; we propose the hydrogenation of adsorbed N_2H_x ($x = 3$, 4). Later in this paper, we will show that

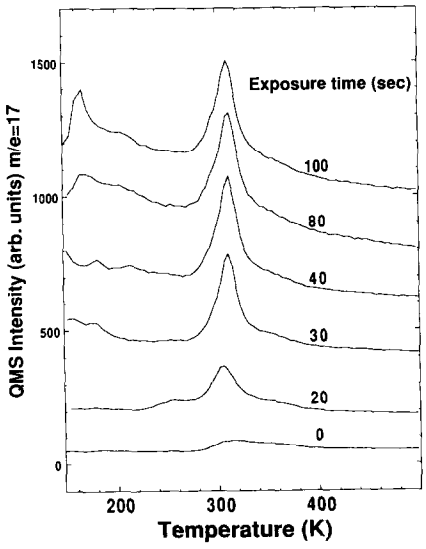

Fig. 4. TPD spectra for NH_3 from various hydrazine exposures on clean Pt(111). Conditions were identical to those of fig. 1.

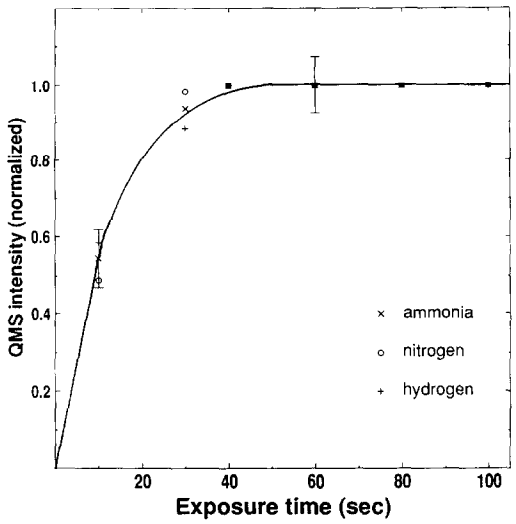

Fig. 5. TPD peak areas, normalized to 100 s exposure, for H_2, NH_3, and N_2 as a function of exposure time. Data taken from figs. 2–4.

there are no NH_3 fragments on the surface, but there are N_2H_x ($x = 3$, 4) fragments which lead to the formation of ammonia. The low temperature 17 amu peak in fig. 4 tracks the multilayer hydrazine desorption and is, thus, attributed to fragmentation of hydrazine in the mass spectrometer ion source.

Each of the TPD spectra for H_2, NH_3, and N_2 has a desorption peak at 310 K and the peak areas versus exposure time (fig. 5) show a common saturation time of 40 s. We propose (see below) that there is a controlling reaction leading to the nearly simultaneous desorption of products.

We also looked for other desorbing species, particularly diimide (N_2H_2), which has been observed from Rh foil over a very broad temperature range beginning at 220 and extending past 400 K [14,24]. Fig. 6 shows 30 and 32 amu spectra from the desorption of N_2H_4. The two faithfully track each other, at all coverages, with relative intensities measured for gas-phase N_2H_4, suggesting that $N_2H_2^+$ is a mass spectrometer cracking fragment of N_2H_4. While there is evidence for adsorbed diimide (see below), it does not desorb in detectable amounts. No other species were detected.

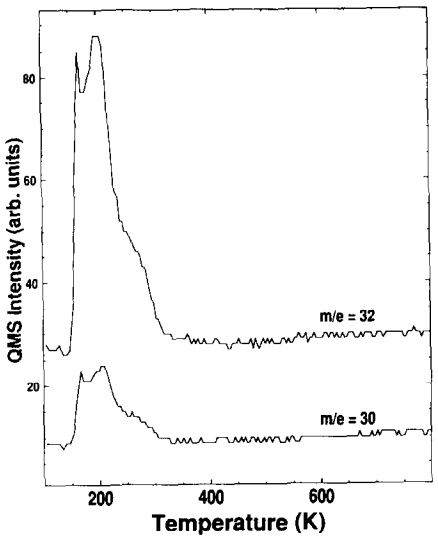

Fig. 6. TPD signals at 30 and 32 amu after adsorption of N_2H_4 on clean Pt(111).

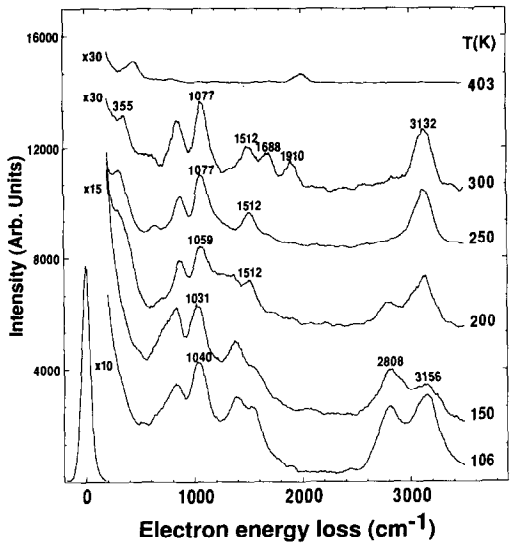

Fig. 7. HREEL spectrum of multilayer N_2H_4 adsorbed on clean Pt(111) at 100 K (lowest curve) and spectra after brief anneal to indicated temperatures (recooled to take spectra).

3.2. HREELS

To assess the vibrational characteristics of the adsorbed species, we measured, at 106 K, HREELS spectra (fig. 7) of multilayer hydrazine before and after annealing to different temperatures. The data are summarized in table 1 along with comparable data for solid N_2H_4 [25], N_2H_4/Ni(111) [8], and NH_3/Pt(111) [26].

The multilayer (106 K) and monolayer (150 K) spectra contain, as anticipated, strong loss peaks assignable to N_2H_4 vibrational modes: e.g., 836 cm^{-1}, NH_2 rock; 1040 cm^{-1}, N–N stretch; 1392 cm^{-1}, NH_2 wag; 1558 cm^{-1}, NH_2 deformation; and 3156 cm^{-1}, NH_2 symmetric stretch (the NH_2 asymmetric stretch was not resolved). Another

Table 1
Summary of HREELS data for solid hydrazine on Pt(111) and Ni(111), ammonia on Pt(111) and IR data for solid hydrazine [a]

N_2H_4/Pt(111)		N_2H_4/Ni(111) [b]	NH_3/Pt(111) [c]	N_2H_4 [d]	Assignment
106 K	300 K	90 K	100 K	IR solid	
–	355	–	350	–	N–Pt
836	855	900	720	884	NH_2 rock
1040	1077	1070	–	1126	N–N stretch
1392	[e]	1340	–	1304	NH_2 wag
–	1512	–	–	–	N–N stretch, bond order $1 < x < 3$
1558	[e]	1580	1630	1603	NH_2 deformation
–	1688	–	–	–	N–N stretch, bond order $1 < x < 3$
–	1910	–	–	–	N–N stretch, bond order $1 < x < 3$
2808	–	–	–	3189	H-bonding
3156	3132	3150	3150	3200	NH_2 symmetrical stretch
[e]	[e]	3300	3320	3310	NH_2 antisymmetrical stretch

[a] Vibrational frequencies (in cm^{-1}).
[b] Ref. [8].
[c] Ref. [26].
[d] Ref. [25].
[e] Not resolved.

relatively strong peak (2808 cm^{-1}) was observed at temperatures through 200 K. Tentatively, this peak is assigned to N–H stretch modes in hydrogen-bonded hydrazine molecules. For hydrazine in solution, the extent of hydrogen bonding increases with concentration and has a characteristic frequency of 3189 cm^{-1} [25].

Above 200 K, the major loss peaks are at 355 cm^{-1}, Pt–N stretching; 855 cm^{-1}, NH_2 rocking; 1077 cm^{-1}, N–N stretching; and 3132 cm^{-1}, NH_2 symmetrical stretching. The persistence of the N–N stretching mode (shifting from 1040 to 1077 cm^{-1}) is evident through 300 K, and, significantly, its relative intensity increases between 200 and 250 K. To account for the increased intensity, we propose that the adsorbed fragment(s) responsible for this loss change their orientation as the sample is heated. For example, changing the N–N bond orientation from a parallel to a tilted (up to perpendicular) orientation to the surface, probably accompanied by N–H cleavage, would increase the cross section for this vibrational excitation.

A new peak at 1512 cm^{-1} appears between 200 and 300 K. We attribute it to adsorbed diimide formed by the loss of hydrogen from hydrazine. From gas-phase UPS spectra, the N–N stretch of diimide has an average value of 1556 cm^{-1} [27]. At 300 K, two additional losses, 1688 and 1910 cm^{-1}, appear and are attributed to other N–N bonded species with a bond order greater than 1 and less than 3. This is based on conclusions from a review by Rao and Rao [28], in which increasing vibrational frequencies have increasing bond order, and from comparisons with the N–N stretching frequencies of azo compounds which lie between 1572 and 1630 cm^{-1} [29].

Above 300 K (fig. 7), no N–Pt stretching frequencies are observed, confirming the complete desorption of all nitrogen-containing species.

3.3. Photoelectron spectroscopy

X-ray photoelectron spectra (figs. 8 and 9) were measured to provide more evidence for changes in the surface atomic composition and chemical environment. Low doses of N_2H_4 at 60 K give a N(1s) BE of 400.2 eV (FWHM = 1.8 eV), whereas multilayer spectra (uppermost curve in fig. 8) give a BE of 400.8 eV (FWHM = 1.8 eV).

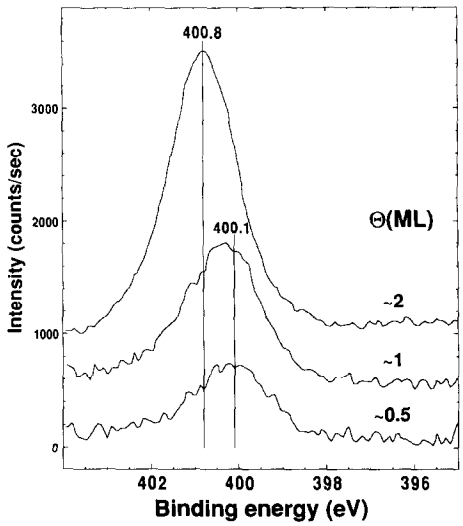

Fig. 8. N(1s) XPS spectra of 0.5, 1, and 2 ML of hydrazine adsorbed Pt(111) at 60 K. An experimentally determined clean surface background has been subtracted from each spectrum.

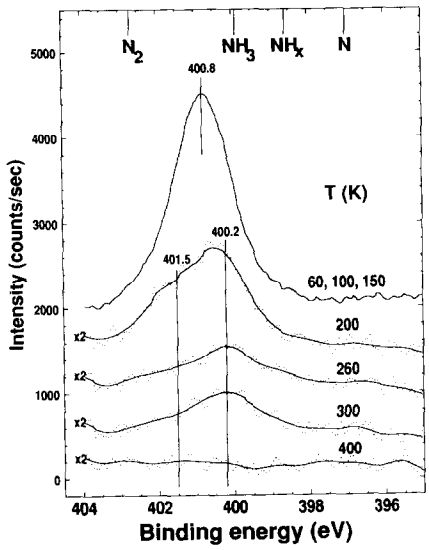

Fig. 9. N(1s) XPS spectra of hydrazine adsorbed on clean Pt(111) at 55 K and subsequently heated briefly to the indicated temperature (recooled to take XP spectrum). The dots are the raw data. The solid line is the result of Fourier smoothing.

These widths are consistent with chemically equivalent nitrogen atoms. Similar binding energy data were determined for monolayer and multilayer N_2H_4 on Fe(111) [4] and on Rh(100) [9].

Annealing 2 ML of N_2H_4, recooling and taking XP spectra leads to the results shown in fig. 9. Importantly, all of the N(1s) signal is gone after a 400 K anneal, confirming that no significant atomic nitrogen concentration is involved. At low temperatures, from 60 to 150 K, the N(1s) intensity and position do not change, i.e., as expected from TPD, multilayer N_2H_4 is preserved. At 200 K, the multilayer has desorbed, and the XP N(1s) intensity is lower and broader, particularly on the higher BE side. This spectrum can be fit with two Gaussian peaks (fig. 10), both with a FWHM of 1.8 eV, centered at 400.2 and 401.5 eV. The inequivalent nitrogen atoms, indicated here, can be interpreted as the sum of contributions from two species: (1) N_2H_x, with one N strongly bound to Pt (lower BE) and one away from the surface (higher BE) and (2) undissociated N_2H_4 with both N atoms bound to Pt (lower BE). Significantly, the higher BE peak is shifted toward N_2 at 402.7 eV [19], not atomic nitrogen at 397 eV, as observed in the case of Fe(111) [4]. An N=N species would be consistent with measurements on azomethane adsorbed on Ag(111) [30]. Thus, XPS is consistent with the HREELS data suggesting that partial decomposition of hydrazine leads to an N_2H_x species with a bond order greater than 1 and less than 3.

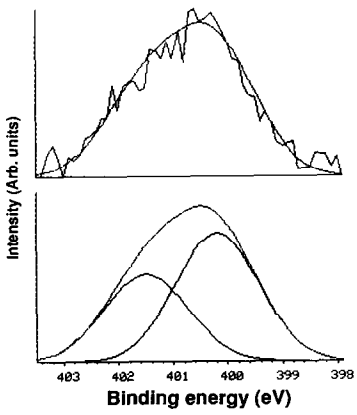

Fig. 10. Deconvolution of the N(1s) peak measured after annealing an N_2H_4 multilayer to 200 K. The deconvolution used two peaks with fixed FWHM of 1.8 eV.

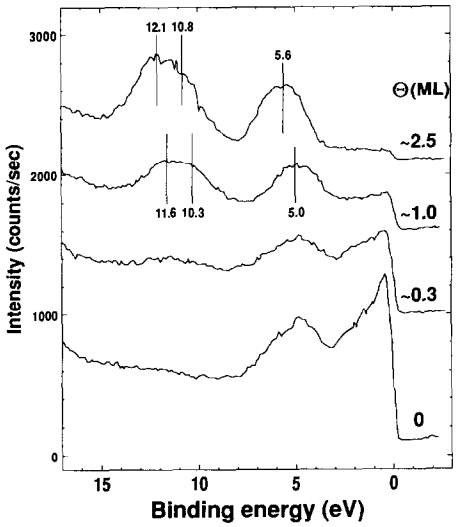

Fig. 11. He(II) UPS spectra of clean, 0.3, 1, and 2.5 ML N_2H_4 adsorbed on clean Pt(111). The three features identified are correlated with those of molecular hydrazine (see text).

Briefly, we consider other N-containing species. NH_3 on Pt(111) has a N(1s) BE at 399.9 eV [18]. NH_x species have N(1s) BE's around 398.6 eV on Al foil [6] and Si(001) [31], whereas atomic N is at 397 eV on Fe [4], Al [32], and Rh(100) [9]. The absence of these peaks on Pt(111) underscores the notion that hydrazine decomposes on Pt(111) by breaking N–H, not N–N, bonds, and that N_2 forms through an intramolecular process, not through atomic recombination.

Fig. 11 shows He(II) spectra for three hydrazine coverages. For 1 ML, peaks were detected at 5.0, 10.3, and 11.6 eV relative to the Fermi level. These are identified with the following molecular orbitals: n_N (4.82, 5.12 eV), σ_{N-N} (10.39 eV), and π_{NH_2} (11.72, 11.91 eV) [33]. Similar UPS peaks were observed on Fe(111) [4], and Rh(100) [9]. As expected for decreased final state screening, all the peaks shift to higher BE (roughly 0.5 eV) when the coverage increases from monolayer to multilayer.

When the multilayer was heated (not shown), the intensity of all the UPS features decreased as they did in XPS. As anticipated, there was no

indication for the retention of a peak at 5.5 eV due to adsorbed N atoms [34].

3.4. TPSIMS

To complement the surface structural data gleaned from XPS and HREELS, we measured temperature programmed secondary ion mass spectra (TPSIMS) under conditions, i.e., static SIMS, where changes due to sputtering were negligible compared to changes due to thermal activation. Fig. 12 shows positive static TPSIM spectra for 17, 18, 32, and 33 amu taken during the heating of multilayer hydrazine. For masses 32 and 33 ($N_2H_4^+$, $N_2N_5^+$), the spectra start to increase at 125 K and reach a local maximum at 145 K. This is due to the desorption of the multilayer hydrazine. All four signals maximize at 195 K, decrease sharply to 240 K, and then decrease slowly, ending at 400 K. The persistence of $N_2H_4^+$ and $N_2N_5^+$ signals to above 250 K lends further support to preservation of N–N bonds to high temperatures. The TPSIMS intensities for NH^+ and NH_2^+ signals at masses 15 and 16 (not shown) were very weak and followed the temporal profiles of the $N_2H_4^+$ and $N_2N_5^+$ peaks. Supporting the XPS and HREELS conclusions that

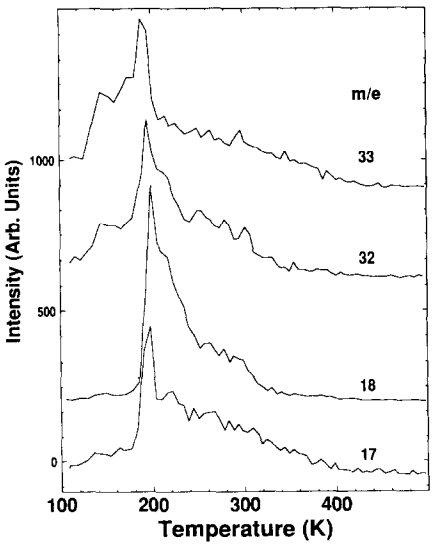

Fig. 12. Positive TPSIMS spectra (17, 18, 32, and 33 amu) for multilayer hydrazine adsorbed on clean Pt(111) at 100 K. The heating rate was 4.5 K/s.

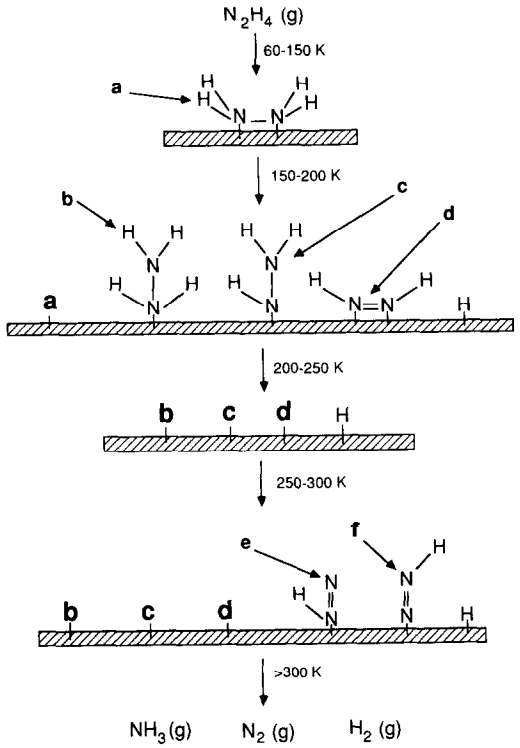

Scheme 1. Schematic of adsorbed intermediates present during thermal processing of chemisorbed hydrazine. Each section lists adsorbed species, thought to be present in significant concentrations. Above 400 K, the surface is clean.

no nitrogen remained above 400 K, we find no SIMS signal for 14 amu, or any other N-containing fragment, above 400 K.

The spectra for mass 17 (NH_3^+) and 18 (NH_4^+) can be attributed either to hydrazine cracking fragments synthesized in the SIMS process or to adsorbed NH_3 formed during the decomposition of the parent molecule. Since the temporal profiles for masses 17 and 18 are nearly identical to those for masses 32 and 33, these results are consistent with the proposal made earlier that neither NH_3 nor NH_2 accumulate, i.e., when N–N bond breaking occurs, NH_3 desorbs.

4. Discussion

To guide the discussion, favored surface structures and relevant temperatures are summarized

in scheme 1. The features are discussed in more detail below.

4.1. Structure of adsorbed hydrazine

Hydrazine is a single bonded nitrogen compound, each nitrogen having sp^3 hybridization, and one lone pair on each N. The geometry is analogous to ethane, with a lone pair on each nitrogen replacing one of the hydrogens on each carbon of ethane. Rotation around the N–N bond is hindered, the rotational barrier lying between 6 and 10 kcal/mol [35,36]. The equilibrium configuration is gauche because of the large dipole moment of the trans (staggered) conformer and because of the coplaner repulsions in the cis (eclipsed) and half cis (semi-eclipsed) conformers.

Intuitively, the lone pairs on the N atoms are likely to be involved in bonding to the Pt(111). Since the N(1s) XPS peak is characteristic of a single type of N atom (400.2 eV BE with a FWHM of 1.8 eV), we favor the di-σ bonded form (species a in scheme 1) in which both N atoms are bound. This conclusion is consistent with that of Grunze on Fe(111) [4].

Considering the distances involved, the di-σ bonded species is reasonable. The nearest-neighbor Pt–Pt bond length is 2.77 Å. In the cis configuration, we estimate 2.4 Å for the distance between the lone pairs, based on a N–N bond length of 1.5 Å [37], an N–N–H bond angle of 108° [37], and an estimated N–lone pair length of 1.014 Å, i.e., the same as the N–H bond length [37]. In the gauche configuration, the distance between the lone pairs will be larger. In this way, hydrazine may be bound to the surface through both lone pairs in a configuration between cis and gauche. As the gauche configuration is approached, the hydrogen atoms will move toward the surface, perhaps lowering the barrier to N–H cleavage. As we discussed above, hydrogen bonding may also exist at monolayer coverages.

4.2. Decomposition of chemisorbed hydrazine

For gaseous hydrazine, the N–N bond energy is 38.4 kcal/mol, whereas N–H is 93.4 kcal/mol [38]. Thus, we anticipated, incorrectly, that the N–N bond would break, giving NH_2, and that this would dissociate to nitrogen and hydrogen adatoms. Instead, on Pt(111), thermal decomposition proceeds by dissociation of the N–H bonds. As outlined below, this may be related to the relatively weak N–Pt bond. At the same time, the Pt–H bond is quite strong (62 kcal/mol [39] derived from the experimental heat of adsorption (19 kcal/mol) of H_2 on Pt(111) [40]).

The relative N–metal bond strengths are related indirectly to the nitrogen recombinative desorption temperatures. On Pt, nitrogen atom recombination (discussed earlier) takes place between 450 and 650 K [20–22]. This may be compared to the following: Rh(111) – 670 K [41]; Rh(100) – 775 K [9], and Fe – 800 K [34]. Therefore, we infer that the relative N–metal bond strengths follow the order: N–Pt < N–Rh < N–Fe. Turning to hydrazine decomposition, we note the following: on Pt, N–H bond dissociation dominates; on Rh, N–H and N–N bond dissociation are both significant; and on Fe, N–N bond dissociation dominates. The following correlation emerges: the stronger the N–metal bond, the more important N–N cleavage becomes.

Upon heating, the hydrazine surface configuration changes (scheme 1). Compared to 150 K, HREELS and XPS spectra have new and/or broader peaks at 200 K. In HREELS, there is a new peak at 1512 cm^{-1}, attributed to diimide (species d). In XPS, the monolayer N(1s) can be deconvoluted into two peaks, i.e., chemically inequivalent N atoms. In addition to residual di-σ bound parent, the XPS is consistent with additional N_2H_x species, e.g., rearranged N_2H_4, N_2H_3 and/or N_2H_2 (species b, c and d, respectively, in scheme 1).

In HREELS the N–N stretching mode also intensifies and shifts to slightly higher wave numbers between 150 and 200 K. We had expected the intensity of this mode to decrease due to the desorption of the multilayer below 200 K. This increase in intensity is attributed to the loss of a hydrogen from hydrazine forming N_2H_3 (species c in scheme 1). A hydrogen atom shift, forming $NH–NH_3$ (not shown), cannot be ruled out. The central feature is the reorientation of the N–N bond with respect to the surface normal. When

N–N lies parallel to the surface, we anticipate a weak HREELS signal because of image charge screening. For monolayer coverages, "standing up" might occur upon N–H cleavage, i.e., N–H cleavage leaves most of the H bound and occupying a site originally occupied by N from hydrazine. Since, on tungsten films, hydrogen blocks adsorption of hydrazine [42], this H-induced rearrangement is possible. These species are present through 300 K.

The new peaks at 1688 and 1910 cm^{-1} in HREELS after annealing to 300 K may be due to other N–N bound species which have a bond order $1 < x < 3$. We tentatively assign these peaks to species e and f as shown in scheme 1. Other evidence for the assignments is the shift to higher BE of the N(1s) XPS, i.e., toward the BE of N_2. Both species are also possible intermediates in the intramolecular N_2 formation, i.e., loss of hydrogen and subsequent changes in the hybridization produces N_2 which immediately desorbs. The loss of the last hydrogen occurs between 275 and 327 K, the observed range of N_2 desorption.

Not all the hydrazine decomposes to form N_2; some ammonia desorbs. As discussed above, we believe it is reaction limited. In related work, Wagner and Schmidt [13] observe two reaction limited desorption peaks for mass 17 after hydrazine adsorption on Rh(111). They attribute the low temperature peak ($T_p = 180$ K) to ammonia from the direct hydrogenation of hydrazine on the surface and the high temperature peak ($T_p =$ 250 K) to ammonia from the hydrogenation of NH_2 species on the surface. On Pt, there is no evidence for NH_2. Therefore, the NH_3 desorption peak is thought to be the result of direct hydrogenation of hydrazine or one of its partially dissociated products (e.g., species c in scheme 1). Tungsten [42], Rh foil [14], and supported iridium [1] substrates behave similarly.

In scheme 1, we have not considered hydrogen bonding interactions. Others have postulated reaction complexes involving two or more N_2H_4 molecules. For example, Wood and Wise [2], have suggested a mechanism, originally postulated by Szwarc [43], by which the nitrogens of N_2H_4 and N_2H_2 species are bound in a square configuration and react to form N_2 and NH_3 by the transfer of hydrogen. This would allow for the simultaneous release of N_2 and NH_3. However, it may be only coincidental that N_2, H_2 and NH_3 all desorb at the same temperature since there are cases where reaction-limited desorption of N_2 formed intramolecularly, and NH_3 formed by direct hydrogenation of hydrazine are observed at different temperatures [8]. There are also cases, similar to that on Pt(111), where N_2 and NH_3 desorb simultaneously [1,5,14].

5. Conclusions

The work reported here can be summarized as follows:

(1) Hydrazine, N_2H_4, adsorbs molecularly on Pt(111) at 60 K. Both nitrogen lone pairs are involved.

(2) Hydrazine desorption occurs in three peaks, a multilayer peak at 165 K, and monolayer peaks at 211 and 270 K. The 270 K peak likely involves hydrogenation of partially decomposed hydrazine. Three reaction products are found in TPD – N_2, NH_3 and H_2 – all desorbing near 310 K.

(3) Thermal decomposition of hydrazine starts between 150 and 200 K and occurs only for those molecules bound to the surface. N–H, not N–N, bonds break and N_2 forms, and desorbs near 310 K, through an intramolecular process. Chemisorption of hydrazine through both nitrogen atoms helps retain the N–N bond and facilitate low temperature N–H bond cleavage. The stronger H–Pt bond, compared to the N–Pt bond, also contributes to preferential cleavage of N–H bonds.

(4) Ammonia is also detected and is attributed to the direct hydrogenation of either N_2H_4 or N_2H_3 species using hydrogen from decomposed hydrazine.

Acknowledgement

This research was supported in part by the US Department of Energy, Office of Basic Energy Sciences.

References

[1] J.P. Contour and G. Pannetier, J. Catal. 24 (1972) 434.
[2] B.J. Wood and H. Wise, J. Catal. 39 (1975) 471.
[3] M.H. Matloob and M.W. Roberts, J. Chem. Res. S (1977) 336.
[4] M. Grunze, Surf. Sci. 81 (1979) 603.
[5] H.H. Sawin and R.P. Merrill, J. Chem. Phys. 73 (1980) 996.
[6] D.W. Johnson and M.W. Roberts, J Electron Spectrosc. Relat. Phenom. 19 (1980) 185.
[7] M. Kiskinova and D.W. Goodman, Surf. Sci. 109 (1981) L555.
[8] J.L. Gland, G.B. Fisher and G.E. Mitchell, Chem. Phys. Lett. 119 (1985) 89.
[9] W.M. Daniel and J.M. White, Surf. Sci. 171 (1986) 289.
[10] D.M. Littrell and B.J. Tatarchuk, J. Vac. Sci. Technol. A 4 (1986) 1608.
[11] D.M. Littrell, D.H. Bowers and B.J. Tatarchuk, J. Chem. Soc. Faraday Trans. I, 83 (1987) 3271.
[12] G.A. Papapolymerou and L.D. Schmidt, Langmuir 3 (1987) 1098.
[13] M.L. Wagner and L.D. Schmidt, Surf. Sci. 257 (1991) 113.
[14] J. Prasad and J.L. Gland, Langmuir 7 (1991) 722.
[15] S.K. Jo, J. Kiss, J.A. Polanco and J.M. White, Surf. Sci. 253 (1991) 233.
[16] G.E. Mitchell, P.L. Radloff, C.M. Greenlief, M.A. Henderson and J.M. White, Surf. Sci. 183 (1987) 403.
[17] J. Kiss, S.K. Jo and J.M. White, to be published.
[18] G.B. Fisher, Chem. Phys. Lett. 79 (1981) 452.
[19] J. Kiss, D. Lennon, S.K. Jo and J.M. White, J. Phys. Chem. 95 (1991) 8054.
[20] K. Schwaha and E. Bechtold, Surf. Sci. 66 (1977) 383.
[21] J. Kiss, A. Berko and F. Solymosi, in: Proc. 8th Int. Vacuum Congr. and 4th Int. Conf. on Solid Surfaces, Eds. D.A. Degrass and M. Costa (Societe Francaise du Vide, Cannes, France, 1980) p. 521.
[22] F. Solymosi and J. Kiss, Surf. Sci. 108 (1981) 641.
[23] K. Christmann, G. Ertl and T. Pignet, Surf. Sci. 54 (1976) 365.
[24] J. Prasad and J.L. Gland, J. Am. Chem. Soc. 113 (1991) 1577.
[25] J.R. Durig, S.F. Bush and E.E. Mercer, J. Chem. Phys. 44 (1966) 4238.
[26] B.A. Sexton and G.E. Mitchell, Surf. Sci. 99 (1980) 523.
[27] D.C. Frost, S.T. Lee, C.A. McDowell and N.P.C. Westwood, J. Chem. Phys. 64 (1976) 4719.
[28] C.N.R. Rao and G.R. Rao, Surf. Sci. Rep. 13 (1991) 221.
[29] CRC Atlas of Spectral Data and Physical Constants for Organic Compounds, Ed. J. G. Grasselli (CRC Press, Cleveland, OH, 1973).
[30] M.E. Castro, L.A. Pressley and J.M. White, Surf. Sci. 256 (1991) 227.
[31] J.L. Bischoff, F. Lutz, D. Bolmont and L. Kubler, Surf. Sci. Lett. 248 (1991) L240.
[32] K. Kishi and M.W. Roberts, Surf. Sci. 62 (1977) 252.
[33] W.L. Jorgensen and L. Salem, The Organic Chemist's Book of Molecular Orbitals (Academic Press, New York, 1973).
[34] F. Bozso, G. Ertl, M. Grunze and M. Weiss, J. Catal. 49 (1977) 18.
[35] H. Ulich and W. Nespital, Z. Phys. Chem. 16 B (1932) 221.
[36] W. Fresenius and J. Karweil, Z. Phys. Chem. B 44 (1939) 1.
[37] G. Herzberg, Spectra of Diatomic Molecules, 2nd ed. (Van Nostrand, New Jersey, 1957) p. 195.
[38] L. Pauling, The Chemical Bond, A Brief Introduction to Modern Structural Chemistry (Cornell University Press, New York, 1967).
[39] E.A. Carter and B.E. Koel, Surf. Sci. 226 (1990) 339.
[40] B. Poelsema, G. Mechtersheimer and G. Comsa, Surf. Sci. 111 (1981) 519.
[41] J. Kiss and F. Solymosi, Surf. Sci. 135 (1983) 241.
[42] R.C. Cosser and F.C. Tompkins, Trans. Faraday Soc. 67 (1971) 526.
[43] M. Szwarc, Proc. R. Soc. London A 198 (1949) 267.